Auxetic Lattice Truss Cores Fabricated of LayWood

Jerzy Smardzewski,* Krzysztof W. Wojciechowski, and Artur Poźniak

Lattice truss cores are used to reduce the mass and increase the strength of sandwich boards. These panels are typically manufactured from metal or carbon composites. As a rule, they do not exhibit auxetic properties. Auxetic structures have several extraordinary mechanical properties. The aim of this study was to manufacture lattice auxetic cores from a biodegradable material and determine their elastic properties. The structures were produced from LayWood Olive, a composite containing polylactic acid and 40% wood dust. The cores had comparable relative densities, but their geometry and number of cells differed. As a result of uniaxial compression in individual lattice truss cores, it was shown that the cores whose cells were square in the top view were isotropic. In contrast, cores with rectangular cells were strongly orthotropic. Moreover, the Poisson's ratio changed depending on the cell size and rib angle. Among the cores that exhibited isotropic properties, the lowest Poisson's ratio and modulus of elasticity were recorded for the structure composed of 49 cells with ribs that were 2 mm thick. The highest Poisson's ratio and modulus of linear elasticity were found with the orthotropic structure composed of 15 cells with ribs that were 3 mm thick. This paper was based on numerical calculations that were verified by experimental studies.

Keywords: Auxetic; Lattice truss cores; LayWood; Experiment; FEM

Contact information: Department of Furniture Design, Faculty of Wood Technology, Poznan University of Life Sciences, Poznan, Poland; Corresponding author: jsmardzewski@up.poznan.pl

INTRODUCTION

Composite sandwich structures are widely used in various fields because of their high specific strength and modulus, high temperature resistance, and damping, *etc.* The cores can be comprised of prismatic elements (honeycomb, textile, and corrugations), an assembly of struts (tetrahedral, pyramidal, and Kagome), or shell elements (egg-box) (Wadley *et al.* 2003). There is additional space in the core to allow the use of a multi-functional filler, which facilitates special engineering applications (Wang *et al*. 2018). Core plates with auxetic properties (*i.e.* having a negative Poisson's ratio) are particularly attractive. Auxetic systems exhibit the unusual and useful property of becoming wider rather than thinner when uniaxially stretched. Grima *et al.* (2013) presented a mechanism to generate auxetic behavior at tailor-made values, which may be implemented in composite manufacture using readily available materials. Huang *et al.* (2017) developed a novel honeycomb design with a negative Poisson's ratio. It was composed of two parts (a reentrant hexagonal component and thin plate) that provided separate contributions to the in-plane and out-of-plane mechanical properties. The authors focused on the in-plane mechanical properties of the auxetic cellular structure. The transverse shear properties of a novel centrosymmetric honeycomb structure were studied by Lira *et al.* (2009). The cellular structure features a representative volume element (RVE) geometry, allowing in-plane auxetic deformations, and multiple topologies to design the honeycomb for multifunctional applications. In contrast, composite sandwich structures with lattice truss

cores have been attracting increasing attention because of their superior specific strength/stiffness and multi-functional applications (Wang *et al.* 2014). Many researchers have emphasized the preferred fabrication methods for these structures and the conceptual basis for topology selection, as well as the attributes of the best load supporting structures. Unfortunately, none of these structures exhibit auxetic properties. Additionally, none of these materials were made of wood or wood composites.

Polymer hierarchical truss materials with low relative densities have been fabricated for compressive tests (Wu *et al.* 2017). The results are very useful for designing ultra-lightweight hierarchical truss materials with high specific strength at low density in order to avoid the deficiencies of this structural configuration. Compressive and shear tests were conducted to investigate the mechanical properties and the failure mechanism of a new composite pyramidal lattice structure made of unidirectional carbon fibre (epoxy laminate). The experimental results show that the new composite has some significant advantages compared with other existing composite pyramidal lattice structures. Wu *et al.* (2016) improved the strength of truss lattice sandwich structures by optimizing the topology structure. As a result the hourglass lattice sandwich structure may be considered as a promising candidate in high specific strength lightweight structures. Xu *et al.* (2016) presented a new method to form graded corrugated truss core sandwich structures based on an auto-cutting and mould-press process. Results showed that the distributions of the truss cores strongly affect bending behavior of sandwich beams. In paper (Wang *et al.* 2018) the authors showed that the mechanical behaviour of the pyramidal lattice truss core sandwich panels made from carbon fibre reinforced composites materials, depends on the relative density of the core and the material properties of truss members. Based upon the previous work (Gao *et al.* 2013) the authors designed and fabricated a strengthened pyramidal truss core with an interlacing laminate form of adjacent nodes to solve the problem of core-separation failure and fully justify the potential of cross-bars. Dong *and* Wadley (2015) investigated octet-truss lattice structures made from balanced [0/90] carbon fiber reinforced polymer (CFRP) laminates using a simple snap-fit method. Their isotropic response may provide new opportunities for ultra-lightweight multiaxial loaded structures. Those authors developed a simple snap-fit and vacuum brazing method to fabricate three-dimensional space filling octet-truss lattice structures from Ti–6Al–4V alloy sheets. These truss lattices exhibit excellent mechanical properties compared to other cellular materials. The study (Xu *et al.* 2015) introduced a novel concept of combining graded material and a lattice truss core to form graded lattice truss core sandwich structures, which is based on the stitching and hot-press process. In the study (Li *et al.* 2011) the mechanical performance of an all-composite pyramidal lattice truss core sandwich structure was investigated. Sandwich structures were fabricated with a hot compression molding method using carbon fibre reinforced composite T700/3234. The pyramidal truss core sandwich structures consisting of CFRP face sheets and aluminum alloy cores were described in the paper (Zhang *et al.* 2013). The aim of this hybrid concept is to maximise the specific bending stiffness/strength as well as provide an excellent energy absorption ability. Pingle *et al.* (2011) developed collapse mechanism maps for the shear response of sandwich panels with a stainless steel core comprising hollow struts. Quasi-static uniform compression tests and low-velocity concentrated impact tests were also conducted to reveal the failure mechanisms and energy absorption capacity of two-layer carbon fibre composite sandwich panels with pyramidal truss cores (Xiong *et al.* 2012).

The literature review shows that layered structures with lattice truss cores are known. These are: corrugated core constructions (Wadley *et al.* 2003), graded corrugated

truss (Xu *et al.* 2015, 2016), two-layer pyramidal truss sandwich core (Xiong *et al.* 2012), pyramidal core (Li *et al.* 2011; Gao *et al.* 2013; Yang *et al.* 2014), hollow pyramidal core with the four tubes (Pingle *et al.* 2011), diamond weave, egg box (Wadley *et al.* 2003), tetrahedral, double layer Kagome 'lattice trusses (Yungwirth *et al.* 2008), 2-D lattice truss core (Wang *et al.* 2014), X-type lattice truss core (Wang *et al.* 2018), octet-truss lattice structures (Dong *et al.* 2015; Dong *and* Wadley 2015). The applied models are distinguished by symmetry and periodicity in two mutually perpendicular directions. Just a few works (Yungwirth *et al.* 2008; Li *et al.* 2011; Xiong *et al.* 2012; Zhang *et al.* 2013l; Feng *et al.* 2016) refer to symmetrical arrangements of pyramidal cores. In these works, the broader base of a single cell is square. This suggests that the cores should have isotropic properties. However, there is a lack of broader discussion of structures with orthotropic properties useful in constructions made of wood or wood-based composites. In addition, the literature review shows that the mechanical properties of sandwich panels with pyramidal cores have been tested many times. They were subjected to bending, compression and shearing. However, the elastic properties of the cores have not been determined. It has not been established whether these are conventional or auxetic structures. The term "auxetic" defines a class of materials that exhibit a negative Poisson's ratio, which causes a counter-intuitive expansion under tension rather than contraction (Evans *et al.* 1991). These materials have been shown to possess enhanced toughness and hardness, as well as absorb sound and vibrations better than their non-auxetic counterparts (Greaves *et al.* 2011). The atypical elastic behavior of auxetic materials is enabling advancements in a broad range of technologies such as high-performance armor, extremely precise sensors, and impact-resistant composites (Alderson 1999). Therefore, it would be important to determine the elastic properties of the lattice core in iso- and orthotropic systems and to demonstrate their auxetic characteristics. In addition, the works discussed were related to structures made of metal, carbon fibers or polymers. The possibility of using them in the design of biomaterial constructions is very limited. They are an additional difficulty in recycling. Therefore, new natural materials are being sought, which can ensure the use of wood-based sandwich panels in the construction.

In fact, the mechanical properties of LayWood are small in relation to metals, carbon fibers or polymers. However, compared to the properties of the paper core, even the auxetic one, the obtained elastic constants are far from being satisfactory (Smardzewski 2013). They can therefore guarantee that multilayered sandwich panel with lattice LayWood core will be distinguished by higher stiffness and strength compared to the honeycomb panels with a paper core.

The aim of this study was to develop new lattice truss core structures with auxetic properties made of wood composite. In particular, it was decided to determine numerically and verify experimentally the elastic properties of the developed structures.

MATERIALS AND METHODS

Models

Five types of lattice truss core models differing in cell shape and size were prepared for the analyses (Fig. 1). Cores A, B, and C are distinguished by periodic geometry in the Cartesian coordinate axes X and Y. Cores D and E are characterised by differing rib slope in the X and Y axes. When selecting the shape, it was decided that cores A, B, and C should exhibit isotropic properties, while cores D and E should be orthotropic. The height of all

cores was identical at H=10 mm. The lattice ribs were 3, 2, 4, 2.5, and 3 mm in thickness for structures type A, B, C, D, and E, respectively. Table 1 also presents relative densities of the modelled structures calculated based on solid models designed using the Autodesk Inventor Professional©. Solid models were printed in the Fused Deposition Modelling (FDM) technology with 3D Flashforge printers (FlashForge Corporation, China) (Fig. 2). The solid X-type print option was applied. The used filament was LayWood Olive (3D Drukujesz, Poland), *i.e.* a composite of PLA and 40% wood dust, with the filament diameter of 1.75 mm and printing temperature of 210 ºC to 220 ºC. During printing, it was used a nozzle with a diameter of 0.1 mm. The thickness of the first layer was equal 0.27 mm and the thickness of next layers 0.14 mm. The temperature of platform was 110 ºC, and the temperature in the extruder 210 ºC. Printing proceeded without the use of supports. For these settings, the average printing time was 15 hours. Five samples were prepared for each model, providing a total number of 25 samples.

Table 1. Relative Cell Density

Core type	Total volume	Volume of the ribs	Relative density
	[mm3]		
A	23040.0	4686.118	0.2034
B	26010.0	5037.276	0.1937
C	31024.9	6634.477	0.2138
D	26676.6	5269.447	0.1975
E	23825.2	4812.807	0.2020

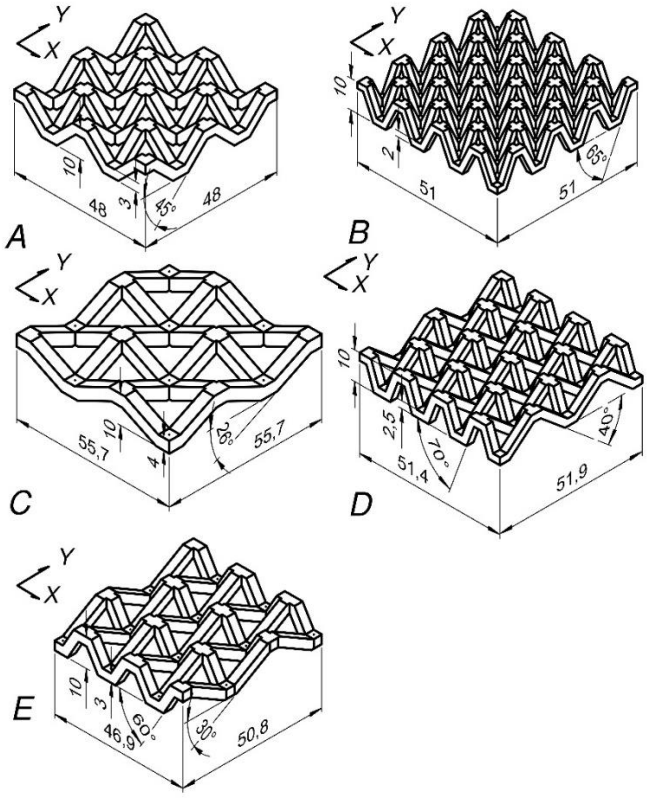

Fig. 1. The shape and dimensions of lattice truss cores

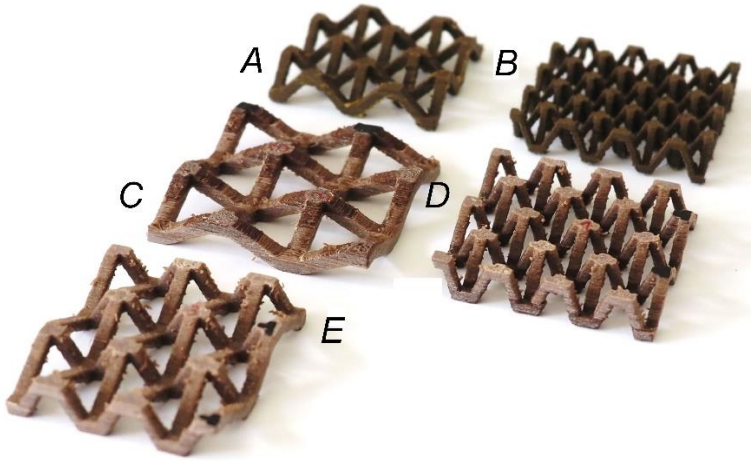

Fig. 2. 3D prints

Materials

Mechanical properties of the filament differ from those of the printed material. For this reason it was decided to determine stress-strain characteristics for the printed material using samples with the shape and dimensions specified in Fig. 3. Samples were printed in the FDM technology using the solid X-type print option. A total of 10 samples were prepared. Samples were subjected to uniaxial tension testing using a Zwick 1445 universal testing machine (Zwick, Germany). Longitudinal and transverse strains were measured by the pattern matching method (Digital Image Correlation) using the Dantec Dynamics system (Dantec Dynamics A/S, Denmark). Based on the recorded direct results, the stress-strain characteristics were plotted for the printed material, while the modulus of linear elasticity and Poisson's ratio were determined (Fig. 4).

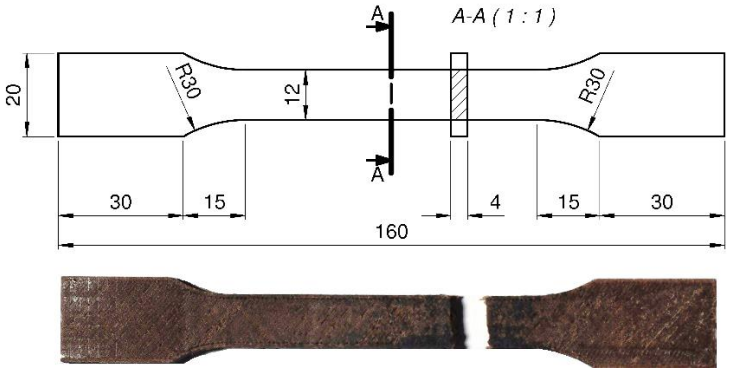

Fig. 3. The shape and dimensions of samples for uniaxial tension testing

In order to include plasticity in numerical calculations for selected cells, the experimental stress-strain dependence had to be converted for LayWood (Fig. 4) after the linear elastic range was exceeded. First the linear elastic range was determined establishing the linear equation for this section. As shown in Fig. 4, the slope of the straight line corresponds to the value of the modulus of linear elasticity for LayWood equal to E_L=601.29 MPa (tensile strength MOR = 10.03 MPa, Poisson's ratio υ=0.36). Next true stress σ_T and the logarithmic plastic strain ε_L, required in the FEM algorithm, were calculated using the equations given below:

$$\varepsilon_L = \varepsilon_T - \left(\frac{\sigma_T}{E_L}\right), \quad (1)$$

where $\sigma_T = \sigma(1+\varepsilon)$, true stress, $\varepsilon_T = ln(1+\varepsilon)$ logarithmic strain, E_L= modulus of elasticity of LayWood, σ = engineering stress, and ε = engineering strain.

For the plastic range in Fig. 4 above the straight line the graph for $\sigma_T = f(\varepsilon_L)$. was plotted. The converted engineering data obtained from the tensile test for LayWood were used to verify their quality. Thus an analogous sample as that in Fig. 4 was modelled in the Abaqus v.6.15 system. The model was ascribed the elastic modulus E_L and respectively determined stresses and strains from the plastic range. Figure 4 presents also tension curves for LayWood samples from experimental tests and numerical calculations. On this basis it was assumed that data conversion was successful and the obtained results are reliable and they were used in further numerical calculations.

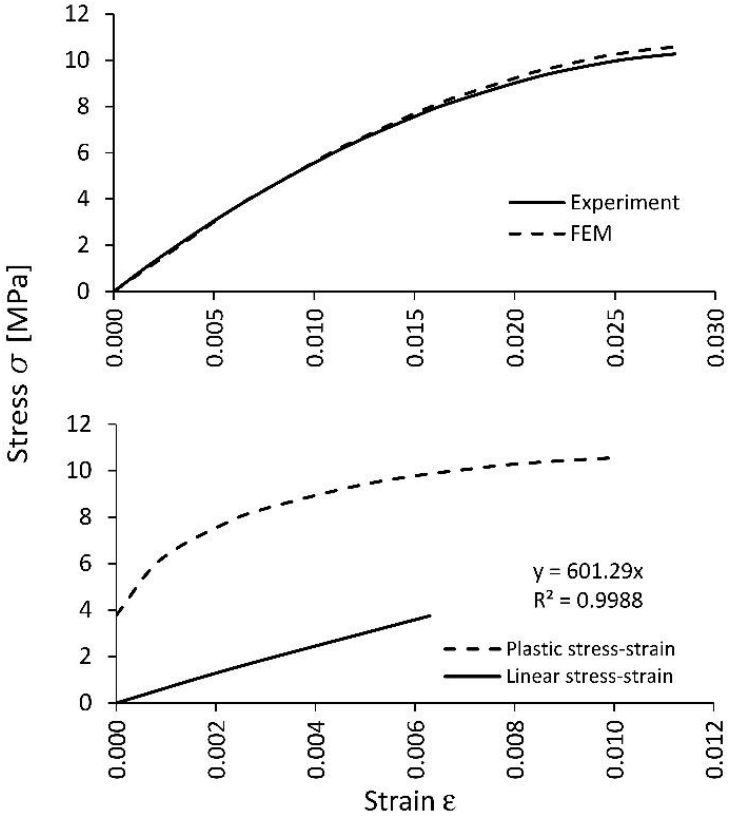

Fig. 4. The stress-strain curve for tensile strength of LayWood

Tests

Printed lattice truss core models were subjected to uniaxial compression in the Y direction and next in the X direction. The diagram for loading and the testing stand are presented in Fig. 5. The tests were conducted using the edge detection method (Digital Image Correlation - DIC) and the IMAQ Vision software (National Instruments, Nederland). Prior to measurements the sample was subjected to preload loading with the force of 5 N. The aim was to eliminate slacks and geometric imperfections of printed structures. Reference images were produced in such a state. Next the load was gradually increased by 10 N accurate to 1 N. For each new value of force one photograph was made. Loads were interrupted when the value of 60 N was reached for the X direction and force

at failure for the Y direction. Based on edge detection (Fig. 6) the digital image analysis method was applied to determine the numbers of pixels in reference sections of 10 mm in length (accurate to 0.02 mm). The same technique was used to measure the length and width of the core before and after strain. Next using the dependencies given below:

$$\nu_{yx} = \frac{dX \cdot Y}{X \cdot dY}, \text{ for the Y direction,} \quad (2)$$

$$\nu_{xy} = \frac{dY \cdot X}{Y \cdot dX}, \text{ for the X direction,} \quad (3)$$

Poisson's ratios υ_{yx}, υ_{xy} were determined, where: dX denotes narrowing, dY elongation, X core width, and Y core length. Moreover, for each of the orthotropic directions the moduli of linear elasticity E_y, E_x were established based on the equations,

$$E_y = \frac{F_y \cdot Y}{H \cdot X \cdot dY}, \text{ for the Y direction,} \quad (4)$$

$$E_x = \frac{F_x \cdot X}{H \cdot Y \cdot dX}, \text{ for the X direction,} \quad (5)$$

where $F_{y,x}$ is the load of the core in the direction of the Y and X axes, respectively, and H denotes core height.

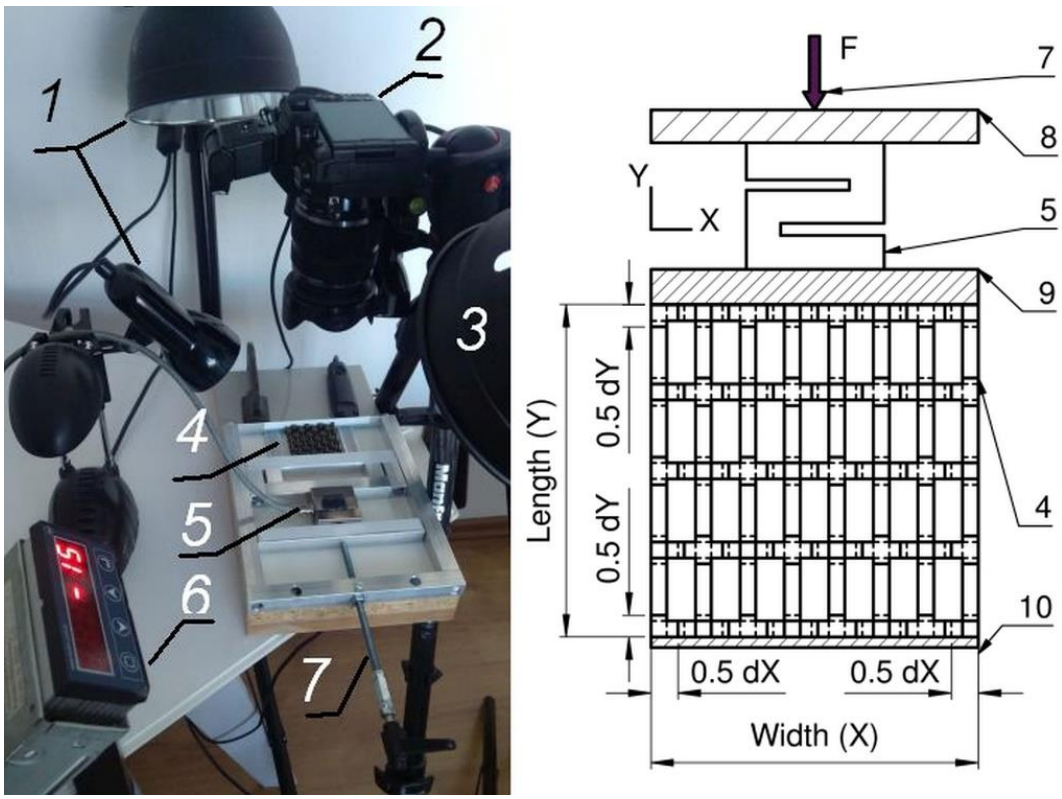

Fig. 5. The stand for measurements of deformation of lattice truss core: 1,3 - reflectors 630 lumens, 2 - Olympus OM-D camera, Olympus, China, 4 - a lattice truss core sample, 5 - PolWobit M12 5kN piezoelectric strain gauge, Poland, 6 - display of piezoelectric strain gauge, 7 - pressure screw (force), 8 - pressure beam of the piezoelectric strain gauge, 9 - pressure beam of samples, 10 – support.

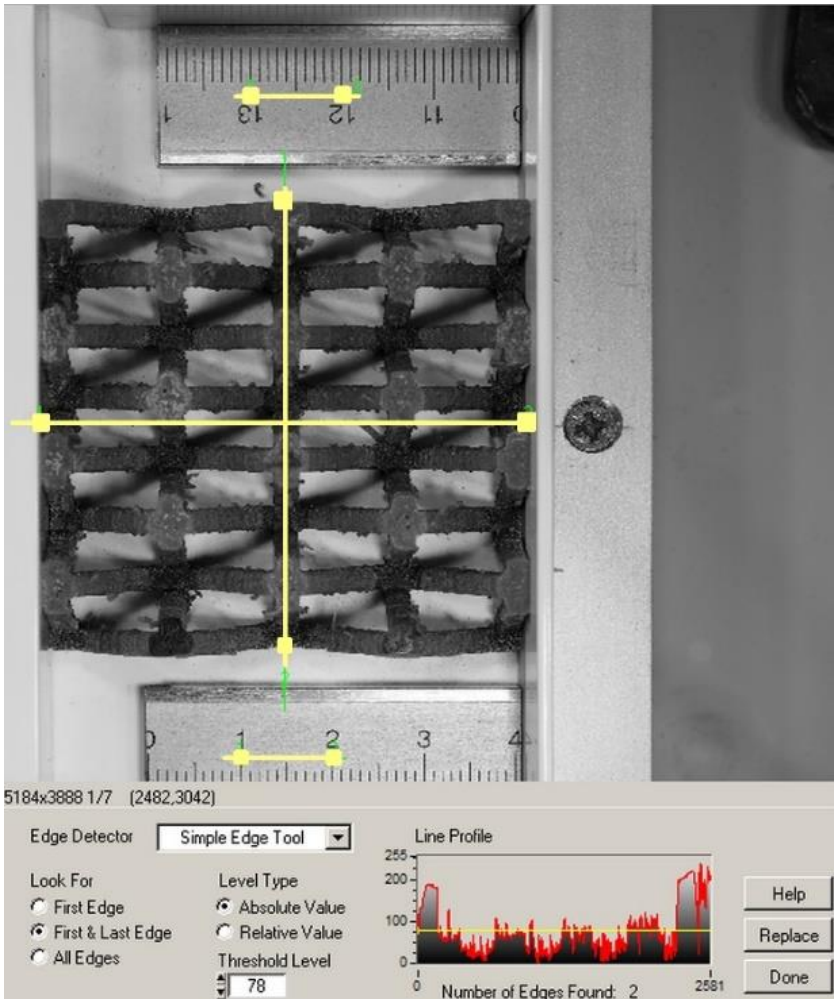

Fig. 6. The method measuring the deformation of lattice truss core

Numerical model

Geometrical models of cell cores prepared with the Autodesk Inventor Professional© system were used to conduct numerical calculations. The files were converted into the STP format and imported to the Abaqus v.6.16 programme. Each core model was ascribed elastic properties of the filament based on the results recorded in the uniaxial tension test. Thus the modulus of linear elasticity and Poisson's ratio for the linear elasticity and respective pairs of numbers representing the stress–strain curve for the plastic strain range were introduced (according to Fig. 4). Figure 7a presents the manner of sample support and loading. It facilitated shifting of unsupported nodes in the direction of the X and Y axes. Modelling was based on a 10-node quadratic tetrahedron element C3D10 (Fig. 7b). Approximately 20.000 elements and approximately 40.000 nodes were applied for each of the models. Load was increased by 10 N following the design adopted for the experimental tests. Based on the recorded displacements, Poisson's ratios υ_{yx}, υ_{xy}, were calculated using Eqs. 2 and 3, while respective moduli of linear elasticity were determined using Eqs. 4 and 5. Computations were performed at the Poznań Supercomputing and Networking Center (PSNC) using the *Eagle* computing cluster.

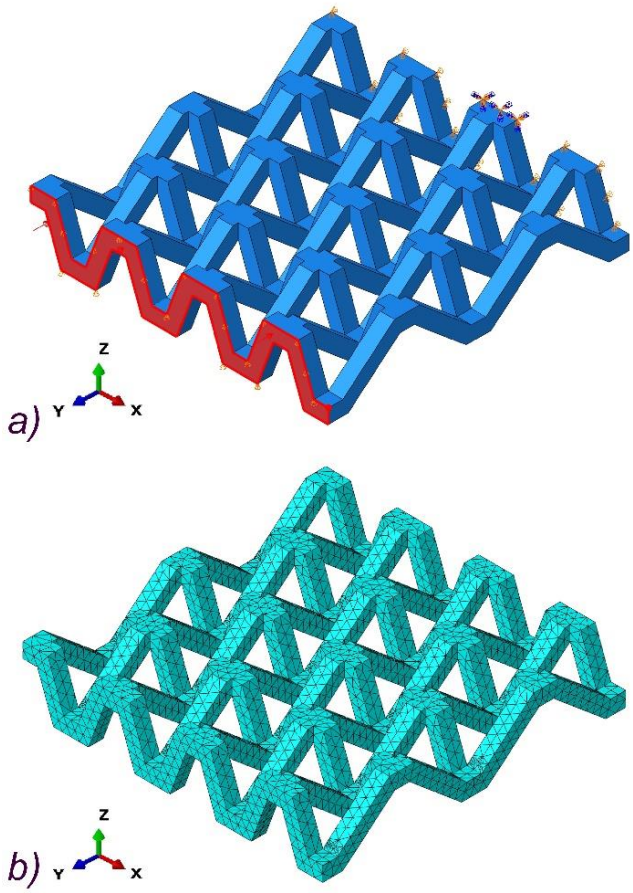

Fig. 7. The static and mesh models of the selected lattice truss core

Statistical analysis

Results of numerical calculations were compared with the experimental testing data. The hypothesis on the significance of differences between the results of numerical calculations and experimental data was verified using Student's t-test for means in independent samples (for $p<0.05$). Analyses were conducted using the Statistica v.13.1 programme.

RESULTS AND DISCUSSION

Results of Numerical Analysis

Figure 8a presents images of deformation for type D lattice truss core subjected to loading with force F_y applied in the direction of the Y axis. These are strains in the direction of the Y and X axes. In turn, Figure 8b shows strains in the Y and X axes for load F_x in the direction of the X axis. The figure indicates that the type D core exhibits strong orthotropy. For load $F_y = F_x$ it shows a greater narrowing dX under load F_y in comparison with narrowing d*Y* for the sample loaded with force F_x. This means that in this case Poisson's ratio υ_{yx} will be many fold greater than υ_{xy}. Similar properties were found for the type E core. In the case of type A, B and C cores numerical calculations showed that they exhibit isotropic properties. Numerical values for these calculations are listed in Table 2.

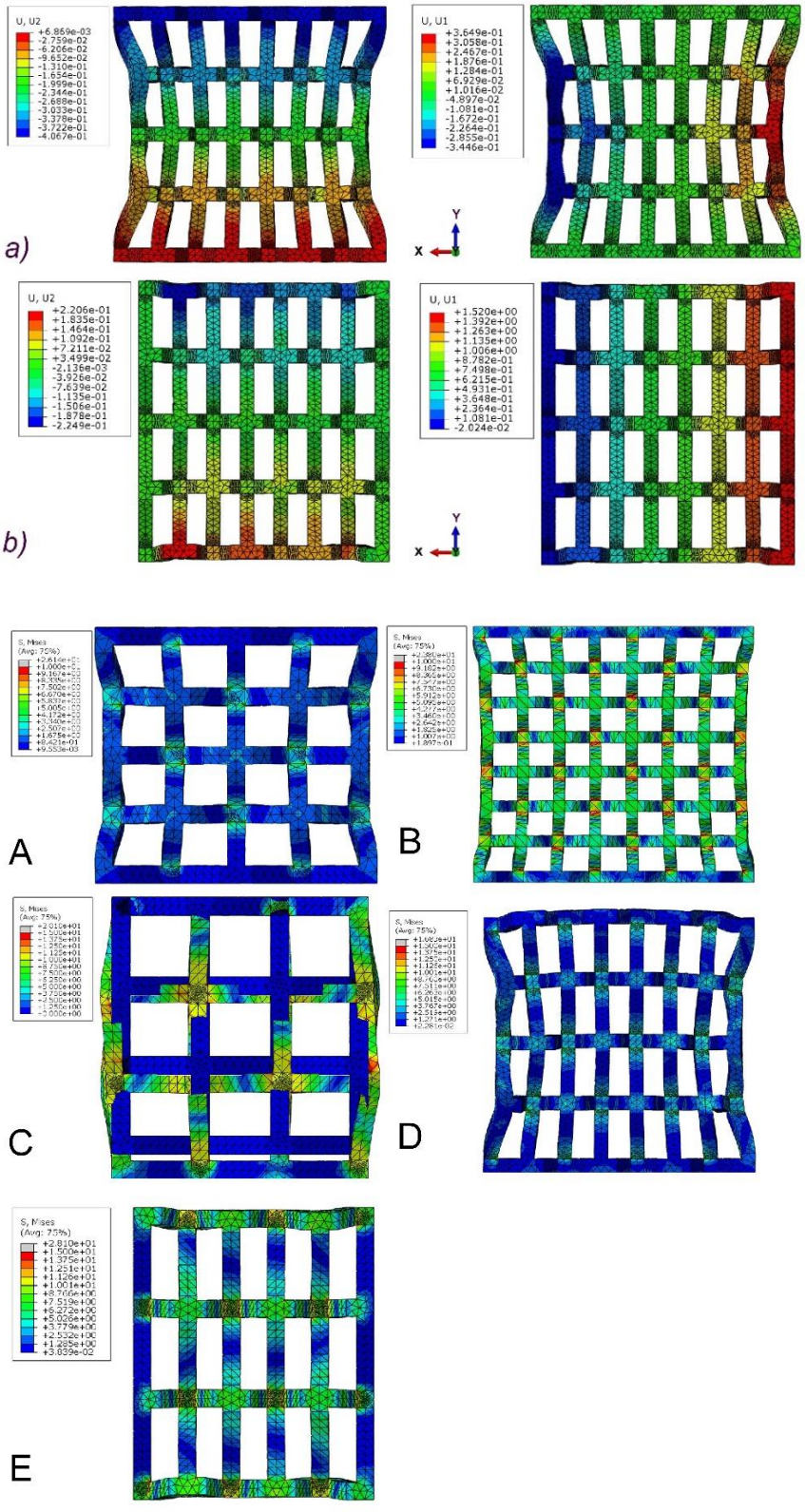

Fig. 8. a,b) Forms of deformation in the selected core (D), c) distribution of the Mises stresses in the cores

Table 2. Elastic Properties of Selected Cores

Core type	FEM				DIC			
	υ_{yx}	υ_{xy}	E_y	E_x	υ_{yx}	υ_{xy}	E_y	E_x
A	-0.6619 (0.0023)	$\upsilon_{xy} = \upsilon_{yx}$	7.99 (0.13)	$E_x = E_y$	-0.6362 (0.0397)	$\upsilon_{xy} = \upsilon_{yx}$	8.48 (0.99)	$E_x = E_y$
B	-0.7535 (0.0070)		2.42 (0.12)		-0.7900 (0.0610)		1.78 (0.25)	
C	-0.5239 (0.0009)		15.75 (0.03)		-0.5197 (0.1147)		15.36 (1.07)	
D	-1.8384 (0.0038)	-0.2035 (0.0055)	18.13 (0.04)	1.96 (0.24)	-1.9167 (0.1043)	-0.0797 (0.0100)	15.04 (0.49)	1.85 (0.01)
E	-1.7859 (0.0045)	-0.1873 (0.0007)	31.95 (0.05)	4.98 (0.41)	-1.3113 (0.2229)	-0.1163 (0.0192)	28.85 (1.46)	3.75 (1.06)

Average (SD)

Table 2 shows that all the numerically modelled lattice truss cores have negative Poisson's ratios. In the case of cores D and E the values of υ_{yx} were less than -1.7. In turn, values of υ_{xy} exceed -0.21. For cores A, B and C Poissons ratios $\upsilon_{yx} = \upsilon_{xy}$ exceeded -0.8. Thus it may be concluded that the modelled lattice truss cores are auxetics. Results of numerical calculations also made it possible to determine values for the respective moduli of linear elasticity. Table 2 shows that core E has the greatest modulus of elasticity for the direction of the Y axis (E_y = 31.95 MPa) and an almost 6-fold lower modulus E_x = 4.98 MPa. In the case of core D the respective moduli are E_y = 18.13 and E_x = 1.96 MPa. Cores A, B and C show isotropy, and thus they have only one modulus of elasticity $E_y = E_x$ of 7.99 MPa, 2.42 MPa and 15.75 MPa, respectively. The results were compared with the experimental testing data in the further part of this paper.

Results of Experimental Tests

The actual dimensions of printed lattice truss cores with auxetic cells were determined based on the digital image analysis (Table 3). These values slightly differ from the model dimensions presented in Fig. 1. The differences may have affected the result of the experiment. Figure 9 presents the stress–strain curves for compressed lattice truss core cells. They indicate that even for small loads the cores are typically deformed non-linearly. This obviously results from the non-linear properties of the applied filament. In addition, this non-linearity is caused by the geometry of the core cells. Cells E, D, and C are the most stocky. They have large ribs thicknesses and relatively small distances between them. Therefore stress–strain curves of these cells have the largest inclination angles to the horizontal axis. In case of cell B, the inclination angle of the curve is the smallest. It is caused by small thickness of the ribs (2 mm). From this reason the stiffness of cells B is very low. The stress-strain curve given in Fig. 9 correctly reflects the strength characteristics of the print. In this case, the stress does not refer to the cross-section of the individual ribs. According to Masters and Evans (1996), the stress in the core is described by the quotient of the force by the area. Area of loading should be equal: for X direction (width X x thickness), for Y direction (width Y x thickness). For the dimensions given in Table 3, it is obvious that stresses have low values. The reduced stresses in the core ribs were determined numerically. Different load conditions were used, both in the direction of

the X axis and the Y axis. The distributions of the Mises stresses are presented in the additional figure 8c. From this figure one can assess that the maximum value of stresses for cells A, B, C, D, and E equal 26.1 MPa, 23.8 MPa, 20.1 MPa, 16.8 MPa, and 28.1 MPa, respectively. Due to the notches, the maximum stresses are concentrated at the points of the arms connection. In the arms, the stresses do not exceed 5 MPa. Taking into account the properties of the developed cores, it can be suggested that they can be used in multilayer wood-based panels.

Table 2 next to numerical calculations presents experimental testing data. Also in this case there is a trend for the lattice truss cores to have negative Poisson's ratios. In the case of cores D and E the value of υ_{yx} is below -1.3 and it is comparable to the results of numerical calculations. In turn, values of υ_{xy} exceed -0.12. For cores A, B and C Poisson's ratios $\upsilon_{yx} = \upsilon_{xy}$ exceed -0.8. Experimental tests has shown that under uniaxial compression, the lateral strains of the A, B, C cores are smaller than the longitudinal strains in the load direction. Therefore, the Poisson's ratios are greater than -1. In case of D and E cells, Poisson's ratios υ_{yx} are less than -1. This means that under uniaxial compression the lateral strains are much greater than the longitudinal. The reverse property occurs for υ_{xy}. In this test, the lateral strains are much smaller than the longitudinal. Since Poisson's ratio are negative in all tests, the lateral strains increase the width of the sample during compression. This provides convincing evidence that all the examined cores are structures with auxetic properties. In this case values of respective moduli of linear elasticity were also determined. It results from Table 2 that core E has the greatest modulus of elasticity for the direction of the Y axis (E_y = 28.85 MPa) and an almost 7-fold lower modulus E_x = 3.75 MPa. In the case of core D respective moduli take the values E_y = 15.04 and E_x = 1.75 MPa. Cores A, B and C show isotropy and as such they have one modulus of elasticity $E_y = E_x$ of 8.48 MPa, 1.78 MPa, and 15.36 MPa. In order to compare the differences, Fig. 10 presents results of numerical calculations together with experimental testing data. They indicate that for most modelled auxetic cores the results of experimental tests were slightly lower than the data from numerical calculations. This difference may stem from the printing quality of physical models. In virtual models the cross-sections of lattice truss ribs were perfectly square. However, elements printed using the FDM technology could not provide such accuracy. For this reason rib cross-sections were only approaching the perfect square outline, typically having rounded or oval edges.

Table 3. Dimensions of the Printed Samples

Core type	Dimensions		
	Length Y	Width X	Thicknes
	[mm]		
A	48.63 (0.59)	48.80 (0.25)	9.86 (0.37)
B	51.14 (0.20)	51.06 (0.14)	10.20 (0.00)
C	56.22 (0.09)	56.03 (0.10)	9.76 (0.05)
D	52.60 (1.01)	50.38 (2.24)	10.02 (0.08)
E	50.91 (0.14)	46.98 (0.11)	10.00 (0.00)

Average (SD)

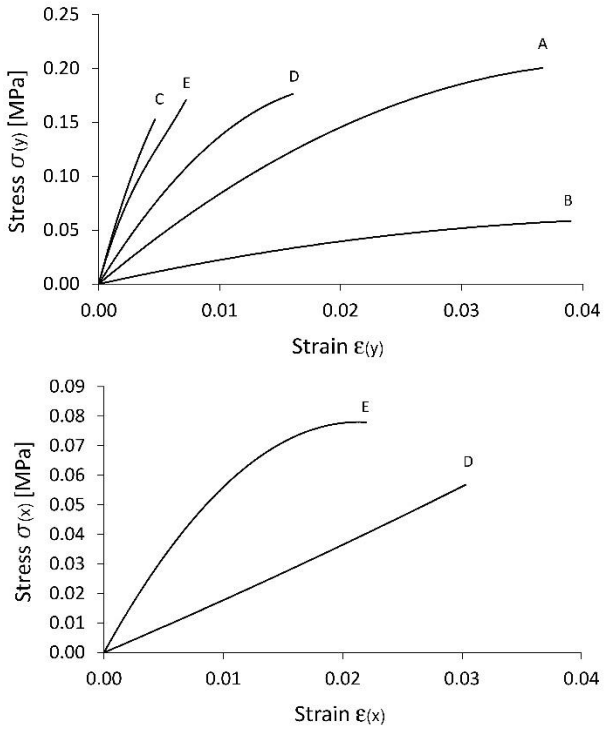

Fig. 9. The stress–strain curve for core with rib (truss) cells

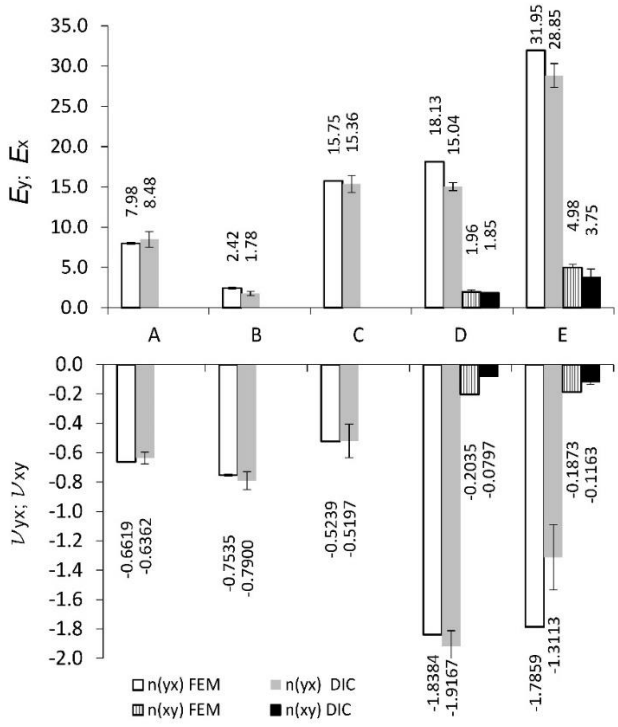

Fig. 10. Elastic properties of selected cores

Nevertheless, it needs to be stressed that the presented models of auxetic lattice cores, at relatively comparable values of relative density ranging from 0.1937 to 0.2138 (Table 1), exhibit considerable variability in terms of their elastic properties. This variability is manifested in the fact that they are iso- and orthotropic structures with negative Poisson's ratios ranging from -0.0797 to -1.9167 and moduli of elasticity within the range from 1.78 MPa to 28.85 MPa.

In the literature there are no results describing auxetic properties of the lattice cores made of various materials. Therefore, the obtained results were compared with the analogous test on paper hexagonal cells. In the work (Huang *et al.* 2017) a negative Poisson's ratio of honeycomb core was described. The core was composed by a part (a reentrant of a hexagonal component and a thin plate part). The authors showed that Poisson's coefficients vary from -0.1 to -4.0 depending on the angle of inclination of the walls.

Statistical Analysis

Table 4 presents results of testing for the hypothesis on the significance of differences between the results of numerical calculations and experimental data. Student's t-test was applied for means in independent samples assuming $p<0.05$. Based on the presented data one may infer the significance of differences only in the case of calculations of values of υ_{xy} and modulus E_y for type A, B, E, and D cores. In the other cases the hypothesis on the significance of differences was rejected, since $p>0.05$. The main reason for differences between the experimental data and FEM prediction for types D and E lies in the quality of the printout. It was observed that physical models diverge from geometry

of computer models. Cross-section of ribs are rather oval than rectangular. This change significantly reduces the mechanical properties of cores. Therefore, the values in the table 2 and 4 obtained by the DIC method are generally smaller than the results calculated numerically. In view of the above it may be assumed that the application of a more accurate printing method should result in a greater consistency in the determination of moduli of elasticity for certain core types.

Table 4. Student's t-test

Core type	Mean DIC	Mean FEM	t	df	p
υ_{yx}					
A	-0. 636208	-0.661917	0.671136	4	0.538898
B	-0.790029	-0.753468	-1.12333	3	0.343080
C	-0.519740	-0.523902	0.048489	5	0.963204
D	-1.91670	-1.83840	-1.06067	2	0.399995
E	-1.31133	-1.78594	2.856206	3	0.064778
υ_{xy}					
D*	-0.079700	-0.203509	15.48993	3	0.000585
E*	-0.116298	-0.187349	7.002054	3	0.005981
E_y					
A*	8.479239	11.38944	-5.22260	4	0.006416
B*	1.779673	2.422382	-4.04416	3	0.027214
C	15.35977	15.75112	-0.486489	4	0.652073
D*	15.03600	18.12663	-8.73084	2	0.012866
E	28.84983	31.95357	-2.85237	3	0.064983
E_x					
D	1.850893	1.961308	-0.755141	3	0.505040
E	3.748801	4.981745	-1.51457	3	0.227115

* Statistically significant difference

CONCLUSIONS

1. Lattice truss cores exhibiting auxetic properties were manufactured from LayWood, a composite containing PLA and 40% wood dust. All of the cores were characterised by comparable relative densities, but they differed in their geometry and number of cells.
2. As a result of the uniaxial compression of individual lattice truss cores, it was observed that cores with cells that were square in the top view were strongly isotropic. The cores with rectangular cells were strongly orthotropic. Moreover, the Poisson's ratio varied depending on the cell size and rib slope.
3. Among the cores with isotropic properties, the lowest Poisson's ratio and modulus of elasticity were recorded with core B, which was composed of 49 cells with ribs 2 mm thick. The highest Poisson's ratio and modulus of linear elasticity were found with core C, which was composed of 9 cells with ribs 4 mm thick.
4. In the group of cores exhibiting orthotropic properties, cores D and E were comprised 28 cells and 15 cells with rib thicknesses of 2.5 mm and 3 mm, respectively. Higher elastic constant values were recorded for core E.

5. The analyses showed that the lattice truss cores manufactured from the biodegradable wood composite exhibited a wide spectrum of elastic properties. Therefore, they may be useful in designing wood-based layered panels. Some particularly promising prospects are connected with the modelling of isotropic or orthotropic structures for such panels depending on the specific application needs.

ACKNOWLEDGMENTS

The present work was conducted as part of the research project no. 2016/21/B/ST8/01016 financed from the funds of the National Science Centre.

REFERENCES CITED

Alderson, A. (1999). "A triumph of lateral thought," *Chem. Indust.* 10(May), 384-391.

Dong, L., Deshpande, V., and Wadley, H. (2015). "Mechanical response of Ti-6Al-4V octet-truss lattice structures," *International Journal of Solids and Structures* 60, 107-124. DOI: 10.1016/j.ijsolstr.2015.02.020

Dong, L., and Wadley, H. (2015). "Mechanical properties of carbon fiber composite octet-truss lattice structures," *Composites Science and Technology* 119, 26-33. DOI: 10.1016/j.compscitech.2015.09.022

Evans, K. E., Nkansah, M. A., Hutchinson, I. J., and Rogers, S. C. (1991). "Molecular network design," *Nature* 353, 124.

Feng, L. J., Wu, L. Z., and Yu, G. C. (2016). "An hourglass truss lattice structure and its mechanical performances," *Materials and Design* 99, 581-591. DOI: 10.1016/j.matdes.2016.03.100

Gao, L., Sun, Y., Cong, L., and Chen, P. (2013). "Mechanical behaviours of composite sandwich panel with strengthened pyramidal truss cores," *Composite Structures* 105, 149-152. DOI: 10.1016/j.compstruct.2013.05.015

Greaves, G. N., Greer, A. L., Lakes, R. S., and Rouxel, T. (2011). "Poisson's ratio and modern materials," *Nature Materials* 10, 823.

Grima, J. N., Cauchi, R., Gatt, R., and Attard, D. (2013). "Honeycomb composites with auxetic out-of-plane characteristics," *Composite Structures* 106, 150-159. DOI: 10.1016/j.compstruct.2013.06.009

Huang, J., Zhang, Q., Scarpa, F., Liu, Y., and Leng, J. (2017). "In-plane elasticity of a novel auxetic honeycomb design," *Composites Part B: Engineering* 110, 72-82. DOI: 10.1016/j.compositesb.2016.11.011

Li, M., Wu, L., Ma, L., Wang, B., and Guan, Z. (2011). "Mechanical response of all-composite pyramidal lattice truss core sandwich structures," *Journal of Materials Science and Technology* 27(6), 570-576. DOI: 10.1016/S1005-0302(11)60110-2

Lira, C., Innocenti, P., and Scarpa, F. (2009). "Transverse elastic shear of auxetic multi re-entrant honeycombs," *Composite Structures* 90(3), 314-322. DOI: 10.1016/j.compstruct.2009.03.009

Masters, I. G., and Evans, K. E. (1996). "Models for the elastic deformation of honeycombs," *Compos. Struc.* 35(4), 403-422. DOI:10.1016/S0263-8223(96)00054-2

Pingle, S. M., Fleck, N. A., Deshpande, V. S., and Wadley, H. N. G. (2011). "Collapse mechanism maps for the hollow pyramidal core of a sandwich panel under transverse

shear," *International Journal of Solids and Structures* 48(25–26), 3417-3430. DOI: 10.1016/j.ijsolstr.2011.08.004

Smardzewski, J. (2013). "Elastic properties of cellular wood panels with hexagonal and auxetic cores," *Holzforschung* 67(1), 87-92. DOI: 10.1515/hf-2012-0055

Wadley, H. N. G., Fleck, N. A., and Evans, A. G. (2003). "Fabrication and structural performance of periodic cellular metal sandwich structures," *Composites Science and Technology* 63(16), 2331–2343. DOI: 10.1016/S0266-3538(03)00266-5

Wang, B., Hu, J. Q., Li, Y. Q., Yao, Y. T., Wang, S. X., and Ma, L. (2018). "Mechanical properties and failure behavior of the sandwich structures with carbon fiber-reinforced X-type lattice truss core," *Composite Structures* 185(October 2017), 619-633. DOI: 10.1016/j.compstruct.2017.11.066

Wang, B., Zhang, G., He, Q., Ma, L., Wu, L., and Feng, J. (2014). "Mechanical behavior of carbon fiber reinforced polymer composite sandwich panels with 2-D lattice truss cores," *Materials and Design* 55, 591-596. DOI: 10.1016/j.matdes.2013.10.025

Wu, Q., Ma, L., Gao, Y., and Xiong, J. (2017). "A new fabrication method for hierarchical truss materials with millimeter-scale struts," *Materials Letters* 186(August 2016), 1-6. DOI: 10.1016/j.matlet.2016.09.024

Wu, Q., Ma, L., Wu, L., and Xiong, J. (2016). "A novel strengthening method for carbon fiber composite lattice truss structures," *Composite Structures* 153, 585-592. DOI: 10.1016/j.compstruct.2016.06.060

Xiong, J., Vaziri, A., Ma, L., Papadopoulos, J., and Wu, L. (2012). "Compression and impact testing of two-layer composite pyramidal-core sandwich panels," *Composite Structures* 94(2), 793-801. DOI: 10.1016/j.compstruct.2011.09.018

Xu, G. D., Zhai, J. J., Zeng, T., Wang, Z. H., Cheng, S., and Fang, D. N. (2015). "Response of composite sandwich beams with graded lattice core," *Composite Structures* 119, 666-676. DOI: 10.1016/j.compstruct.2014.09.042

Xu, G., Yang, F., Zeng, T., Cheng, S., and Wang, Z. (2016). "Bending behavior of graded corrugated truss core composite sandwich beams," *Composite Structures* 138, 342-351. DOI: 10.1016/j.compstruct.2015.11.057

Yang, J., Xiong, J., Ma, L., Zhang, G., Wang, X., and Wu, L. (2014). "Study on vibration damping of composite sandwich cylindrical shell with pyramidal truss-like cores," *Composite Structures* 117(1), 362-372. DOI: 10.1016/j.compstruct.2014.06.042

Yungwirth, C. J., Wadley, H. N. G., O'Connor, J. H., Zakraysek, A. J., and Deshpande, V. S. (2008). "Impact response of sandwich plates with a pyramidal lattice core," *International Journal of Impact Engineering* 35(8), 920-936. DOI: 10.1016/j.ijimpeng.2007.07.001

Zhang, G., Wang, B., Ma, L., Xiong, J., and Wu, L. (2013). "Response of sandwich structures with pyramidal truss cores under the compression and impact loading," *Composite Structures* 100, 451-463. DOI: 10.1016/j.compstruct.2013.01.012

Article submitted: August 1, 2018; Peer review completed: September 30, 2018; Revised version received: October 11, 2018; Accepted: October 12, 2018; Published: October 22, 2018.
DOI: 10.15376/biores.13.4.8823-8838